

Comparative investigation on the thermal degradation and stabilization of carbon fiber precursors

Gang-Ping Wu · Chun-Xiang Lu · Li-Cheng Ling · Yong-Gen Lu

Received: 21 October 2008 / Revised: 30 December 2008 / Accepted: 9 January 2009 /
Published online: 25 January 2009
© Springer-Verlag 2009

Abstract Thermal degradation and stabilization of two kinds of polyacrylonitrile (PAN) fibers have been investigated by a combination of FT-IR, differential scanning calorimetry (DSC), modulated DSC, thermogravimetry (TG), thermal shrinkage behavior, in situ mass spectrometry (MS), and tensile property examinations. The two types of precursor fibers exhibit distinct properties after oxidative stabilization, but they can both make carbon fibers with equivalent mechanical properties. Compared with PAN/itaconic acid precursor fibers, the fibers containing acrylamide comonomers show a doublet appearance, broader exothermic peak, lower threshold degradation temperature, and more amount of heat evolved in DSC thermogram, which is favorable to obtain uniform microstructures in oxidative stabilization process. The two types of samples produce different ring structures in the thermal degradation and stabilization process, as evidenced by results from tensile test, TG–MS and thermal shrinkage behavior analyses. In addition, the molecular rearrangement or melting of ordered structures accompanying with nitrile polymerization was also detected from modulated DSC.

Keywords Carbon fibers · Polyacrylonitrile · Degradation · Stabilization

G.-P. Wu · C.-X. Lu (✉)

Key Laboratory of Carbon Materials, Institute of Coal Chemistry,
Chinese Academy of Sciences, 030001 Taiyuan, Shanxi, China
e-mail: lucx@sxicc.ac.cn

G.-P. Wu
e-mail: wgp@sxicc.ac.cn

L.-C. Ling
College of Chemical Engineering and Technology,
East China University of Science and Technology, 200237 Shanghai, China

Y.-G. Lu
College of Material Science and Engineering, Donghua University,
201620 Shanghai, China

Introduction

Thermal degradation and stabilization of polyacrylonitrile (PAN) have been the subject of extensive research since the 1960s [1]. Most activities were centered on the physical and chemical changes [2–8]. The physical changes include color, crystallinity, entropy, density, and tensile strength; while chemical changes include nitrile polymerization, chain scission, evolution of volatile gases (NH_3 , CH_4 , CO , CO_2 , H_2O , and so on), and formation of carbonyl, carboxyl, and peroxide groups. Now it has been widely accepted [9, 10] that high quality PAN precursor fiber is a significant prerequisite for obtaining high-performance carbon fibers; however, it is not fully clear what is the ideal precursor structure appropriate for making high-performance carbon fibers. In this study, thermal degradation and stabilization of two kinds of PAN fibers were carried out. The as-stabilized fibers exhibit distinct differences in mechanical properties, but they exhibit equivalent mechanical properties of carbon fibers. A combination of FT-IR, differential scanning calorimetry (DSC), modulated DSC, thermogravimetry (TG), in situ mass spectrometry (MS), and thermal shrinkage behaviors were performed to reveal the difference in the degradation and stabilization process for the two types of fibers. Analyzing these differences may provide useful information for fabricating high quality PAN precursor fibers that is more favorable for thermal stabilization and for obtaining high performance carbon fibers.

Experimental

Materials

Two kinds of PAN precursor fibers were used in this work. Fibers P1 were wet spun by extruding acrylonitrile/itaconic acid (AN/ITA 99/1 wt %) copolymer solution into dimethylsulfoxide (DMSO) coagulation bath. Fibers P2 were supplied by Mitsubishi Rayon Company. Both fibers contain 3,000 filaments in each single tow. The properties were listed in Table 1.

Thermal stabilization and carbonization

The thermal stabilization and carbonization were carried out in a self-designed continuous production line.

Table 1 Properties of PAN fibers

PAN fibers	Tensile strength (GPa)	Elastic modulus (GPa)	Elongation at failure (%)	Density (g/cm^3)	Crystallinity (%)	Orientation index (%)
P1	0.46	6.7	12.79	1.182	35.3	82.9
P2	0.53	8.6	10.63	1.186	43.9	88.3

Measurements and characterizations

The carbon, oxygen, and hydrogen contents in the precursor fibers were measured by a Vario EL III elemental analyzer. FT-IR spectra were recorded from KBr pellets over the range 4,000–400 cm^{-1} using a Perkin-Elmer instruments.

Simultaneous thermal analysis for differential scanning calorimetric analysis and thermogravimetric analysis were carried out in NETZSCH STA 409PC, with purged atmosphere gases, air or nitrogen.

Modulated DSC experiments were performed in air using a Model 2910 Modulated DSC. The heating rate and the cooling rate were 10 and 5 $^{\circ}\text{C}/\text{min}$, respectively. Every thermogram was repeated at least twice, and a duplicate blend was then analyzed to verify the reproducibility of the measurement.

The thermogravimetric analysis coupled with mass spectroscopy (TG–MS) was carried out in air on SETARAM TG-92 instrument and OMNISTAR 200 quadrupole mass spectrometer. The samples were heated from room temperature to 400 $^{\circ}\text{C}$, with heating rate of 1 $^{\circ}\text{C}/\text{min}$.

In order to understand the difference in the two types of precursors, the fiber length changes under constant tensile load were trace-recorded by self-made instrument during a continuous heating of PAN fibers in air.

Mechanical properties, tensile strength, elastic modulus and elongation to failure were tested by a testing machine with a cross head speed of 1 mm/min and a gauge length of 20 mm. Diameters of the fibers were determined under an optical microscope. Mechanical properties and diameters were determined by averaging at least 30 measurements on individual filaments.

A Rigaku X-ray powder diffractometer with CuK_α radiation as a source was used to study the wide-angle diffraction pattern (X-ray wavelength, $\lambda = 0.15418$ nm). The diffraction patterns were analyzed using MDI Jade 5.0. Crystallinity was determined by de-convoluting the integrated WAXD patterns and by using the ratio of the crystalline peaks to the total area. Orientation index of the PAN crystal was determined using the azimuthal scans at 2θ of 17° , in conjunction with the following equation:

$$\text{Orientation index}(\%) = \frac{180 - H}{180} \times 100\% \quad (1)$$

where H is the full-width at half the maximum intensity (FWHM), which was estimated from the peak of azimuthal scan.

Results and discussion

Differences in structures and properties of precursor fibers

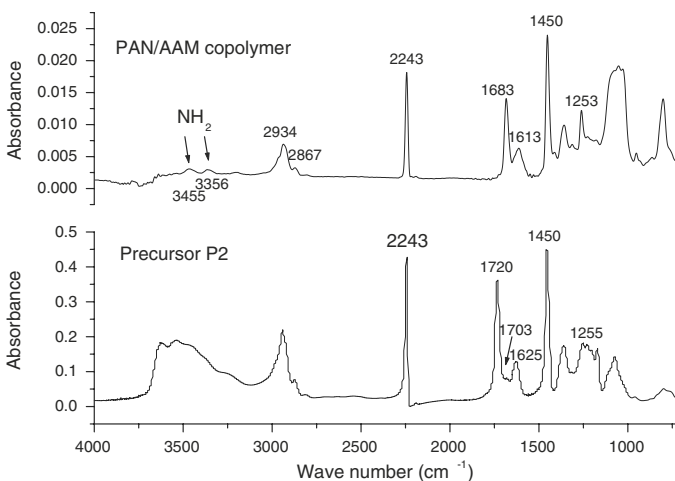
Table 2 presents the elemental compositions for precursor P1 and P2. As shown in the Table, precursor fibers P2 gives higher nitrogen content and somewhat lower oxygen content than P1, suggesting that there may different comonomers contained in the two types of PAN fibers.

Table 2 Elemental compositions of precursor P1 and P2

Precursor	Elements			
	Carbon (wt %)	Oxygen (wt %)	Hydrogen (wt %)	Nitrogen (wt %)
P1	66.64	3.07	5.71	24.58
P2	66.78	1.73	5.72	25.77

Zhang et al. [11] have ever deduced that precursor P2 contain acrylamide comonomers. A comparison of the FT-IR spectra for precursor P2 and PAN/AAM copolymer is shown in Fig. 1. It can be seen that the characteristic vibrations of amide groups [12] are similar in FT-IR spectra, i.e., amide I absorption band ($1,599\text{--}1,710\text{ cm}^{-1}$) and amide II band ($1,483\text{--}1,595\text{ cm}^{-1}$) were observed in P2 samples. In addition, the FT-IR spectrum of the P2 sample shows a strong band at around $3,500\text{ cm}^{-1}$ that is associated with the O–H stretching vibration of hydrogen bonded molecules. The band, along with C–O stretching vibrations ($1,250\text{--}1,150\text{ cm}^{-1}$), suggest that there may other comonomers in the sample, such as ester. The conclusion is consistent with that of Zhang et al.

The two types of PAN fibers have normal stress–strain curve distributions (as shown in Fig. 2), like most textile fibers [13]. The coefficient of variation (CV) of the tenacity, modulus and elongation of the fibers in the yarn is lower than 10%. Compared with P1 fibers, the P2 fibers exhibit a larger tenacity and modulus, but show a lower elongation, as displayed in Table 1. This may be due to the change of the stretching ratio which leads to a change in the macromolecular arrangement. Table 1 show that precursor P2 has larger crystal size and orientation degree than P1. It has been well accepted that the tenacity and elastic modulus of PAN fibers are controlled by the degree of orientation of molecular chains in the fiber axis direction

**Fig. 1** Comparison of FT-IR pattern for precursor P2 with PAN with acrylamide copolymer

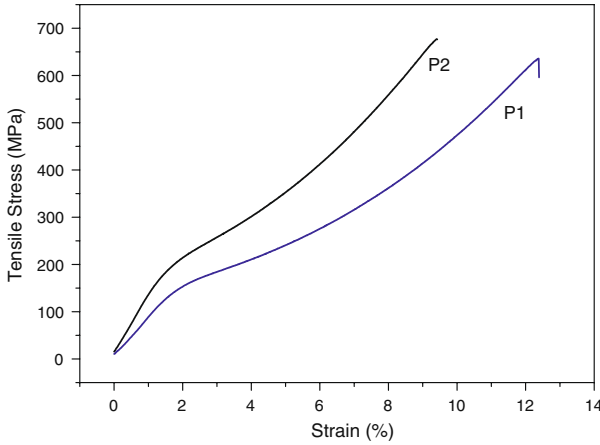


Fig. 2 Axially tensile stress–strain curves of precursor fiber P1 and P2

as well as the size of crystallites, thus it can be concluded that the differences in properties are due to the structural variation induced by stretching on spinning.

Evaluation on thermal stabilization and degradation of PAN fibers

The changes in thermal shrinkages during stabilization as a function of heating temperature are shown in Fig. 3. Both fibers P1 and P2 shrink in length on application of a load of 0.1 g/filament with increasing temperature. Fibers P2 showed an overall shrinkage of 9.2% up to 250 °C, which is two times as larger as that of fibers P1. The shrinkage in fibers P2 pick up very fast above 125 °C and reach a plateau at about 160 °C, followed by a quick increase above 208 °C; whereas in fibers P1, most shrinkage occurred in the 220–250 °C temperature range.

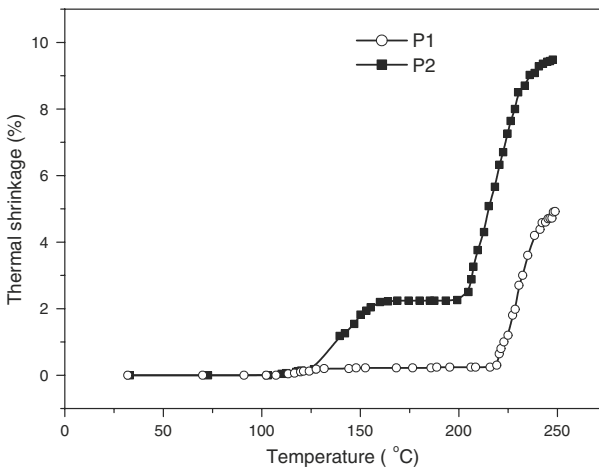


Fig. 3 Change in thermal shrinkage with temperature for precursor fibers P1 and P2

In the temperature region 125–200 °C, the thermal shrinkage is deemed as molecular physical relaxation; however, the shrinkage occurs beyond 200 °C in both fibers because of the onset of cyclization reactions [14, 15]. The P1 fiber demonstrates a very small physical shrinkage, indicating that the molecular orientation in the fiber is maintained and backbone chain sliding is prevented. It is worth noting that fibers P2 exhibits a chemical shrinkage (200–250 °C) of 7% whereas only about 4.7% for fibers Bahl et al. have ever reported [3, 8] that shrinkage in PAN fibers occurs as a result of cyclization upon heating, and it even be used for kinetic study of cyclization reaction by some authors [15]. Thus it is very possible that fibers P2 have a greater degree of cyclization than fibers P1.

Figures 4 and 5 correspond to the DSC profiles carried out under nitrogen and air atmosphere. The precursor P2 give prominent doublet exothermic peaks situated at about 249.6 and 270.3 °C in nitrogen on the DSC thermogram, whereas precursor P1 only exhibit a single exothermic peak at around 280.5 °C. If a change of heating atmosphere occurs from nitrogen to air, all the DSC exothermic thresholds and peak temperatures have been significantly decreased, and the enthalpy calculated from the area under the peak has also got increased. Obviously, the increased enthalpy should be due to the oxidation or dehydrogenation. It is apparent that a combination of cyclization and oxidation/dehydrogenation has turned PAN linear macromolecule into ladder structure and strengthened its thermal stability [16].

As shown in the Figures, the fibers P2 show a doublet appearance, broader exothermic peak, lower threshold degradation temperature, and more amount of heat evolved as compared with those of fibers P1. It seems that nitrile cyclization in P2 is affected by the incorporating acrylamide. One possible reason is that the initiation mechanism in fibers P2 is different from that of P1, as proposed by Sivy et al. [17]. This seems can be further verified by the weight loss behaviors of the two types of samples. A steep sloop in sample P1 (shown in Fig. 6) indicates the intense nitrile reactions of fibers P2 from 236–350 °C, while the weight loss of fibers P2 seems more gradually.

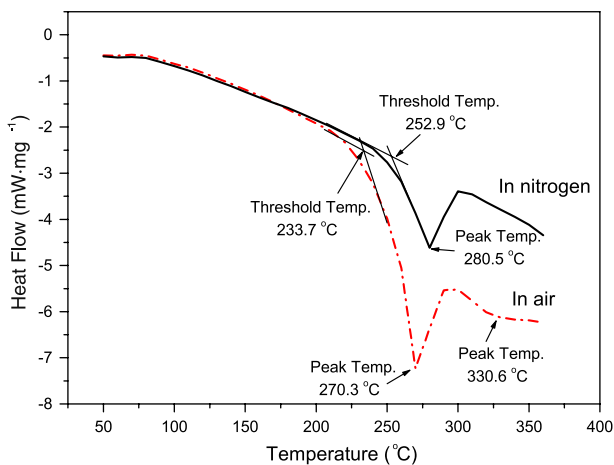


Fig. 4 DSC patterns of precursor fibers P1

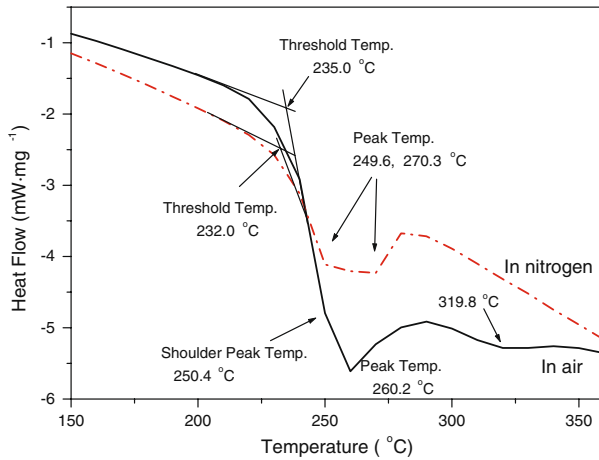


Fig. 5 DSC patterns of precursor fibers P2

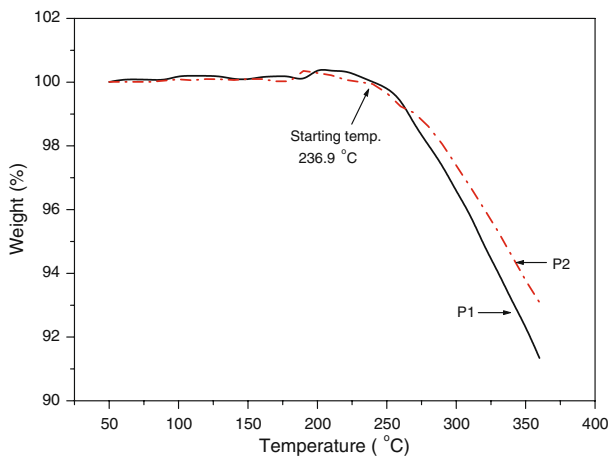


Fig. 6 TG patterns of precursor fibers in nitrogen

The results detected from modulated DSC test for P1 and P2 samples are shown in Figs. 7 and 8, respectively. The thermal response behaviors are indicated by the reversing, non-reversing and loss heat capacity curves. Both P1 and P2 samples give a small endothermic peak above 250 °C in the reversing curves. Conversely, the non-reversing curve of P2 sample contained a distinct exothermic peak at about 267.8 °C and a shoulder at around 284.8 °C on the higher temperature side, followed by an exothermic peak around 327.1 °C which is associated with the formation of large, cross-linked aromatic molecules. The non-reversing curve of P1 sample provide a similar exothermic at 284.5 °C; however, the shoulder exothermic peak is absent. Obviously, the P2 sample has a lower onset temperature than P1 sample, possibly on account of the doublet peaks in DSC thermogram of P2 fibers.

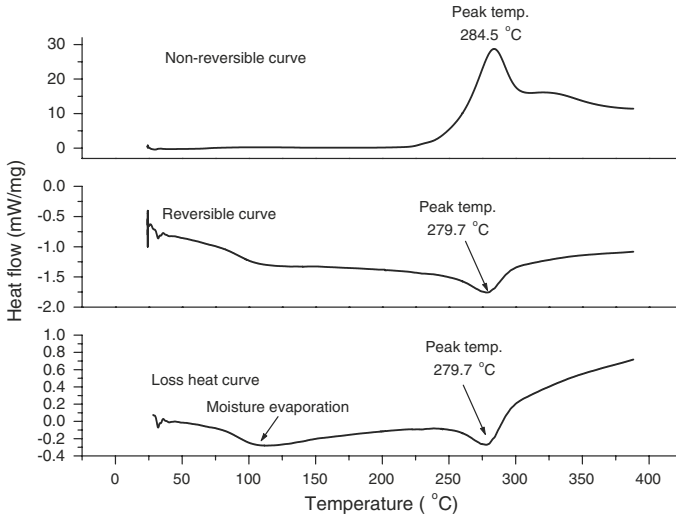


Fig. 7 Modulated DSC patterns of samples P1

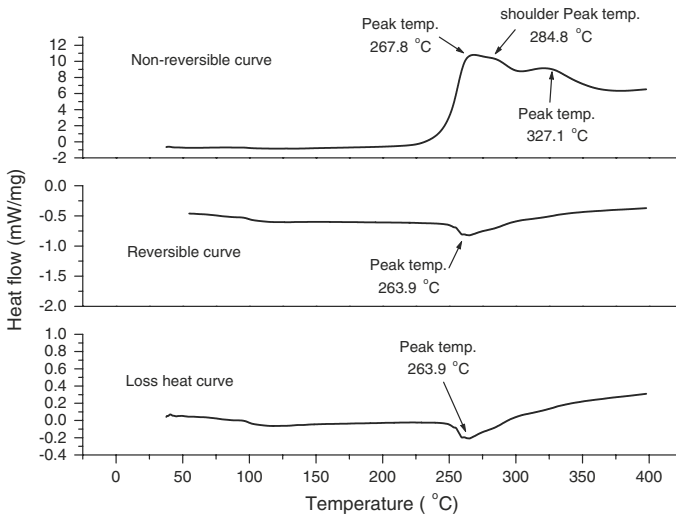


Fig. 8 Modulated DSC patterns of samples P2

The low temperature onset of cyclization is an important precondition for obtaining stabilized fibers with uniform microstructures, as suggested by Yu et al. [9].

The reversing heat capacity contains the reversible component of the total heat capacity, while the non-reversing signal represents the irreversible component of the total heat capacity under the modulation. The presence of an exothermic non-reversing contribution suggested that the samples experienced significant nitrile reactions in the heating process, whereas the endothermic reversing contribution above 250 °C is due to molecular rearrangement or melting of crystalline

component. It is often not possible to detect the structural changes in conventional DSC due to the superposition of a reacting exotherm and a melting endotherm. The reversing curves pertaining to crystal melting is conformed by Raskovic et al. [18], that is, they found that PAN homopolymer fibers would show a significant endotherm at this temperatures by differential thermal analysis.

The presence of small reversing contributions along with large exothermic irreversible contributions confirmed the formation of thermally stable cyclized structures during the structural changes. The loss specific heat curves, which also represents the reversible contribution. Except for a small endothermic contribution associated with moisture evaporation, these loss heat curves show zero baselines up to 250 °C, suggesting there were no physical changes involved before that temperature.

In the temperature region of 250–300 °C, the irreversible exothermic peak with a shoulder is analogous to the doublet peaks in conventional DSC for P2 sample. Gupta et al. [19] have ever reported that the doublet peaks are corresponding to the stabilization reactions in amorphous and crystalline regions, respectively. Thus it is conclusive that the first exothermic peak which is previously deemed to be associated with amorphous stabilization conceals a reversible molecular rearrangement, whereas the second exothermic peak which is deemed to be associated with stabilization reactions in crystalline region conceals a reversible melting in crystalline structures. This is consistent with the stabilization mechanism of PAN proposed by Ko et al. [20].

TG–MS are useful techniques employed to characterize the thermal decomposition of PAN fibers. During TG–MS experiments, the releasing products from samples are simultaneously and continuously monitored by MS, as shown in Fig. 9, the major products from decomposition of samples include H₂O, CO, CO₂, CH₄,

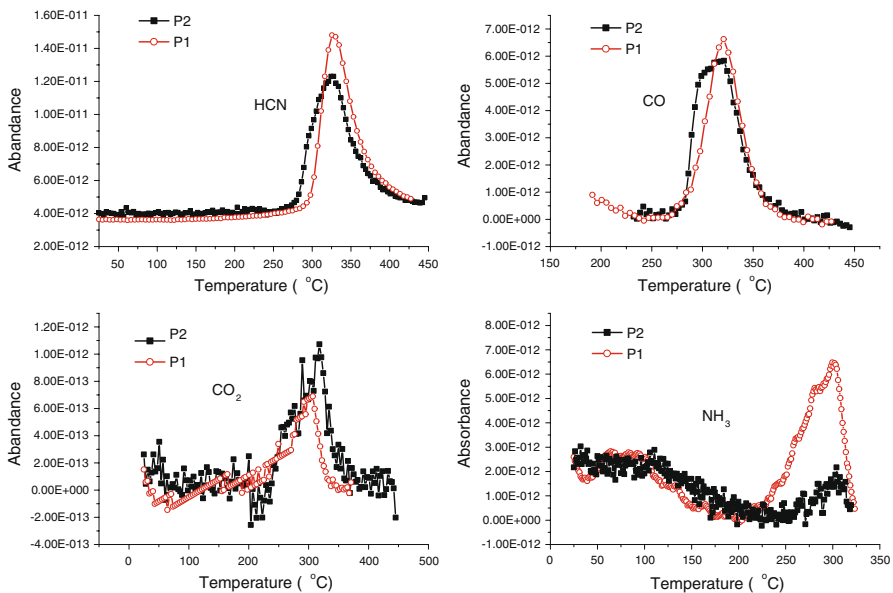


Fig. 9 Abundance of the major evolved gases from the TG-MS analysis of PAN fibers

NH₃, HCN and some aromatic derivatives. As shown in Fig. 9, a slight difference was apparent in the abundance of CO, CO₂ and HCN volatiles, however, distinct local differences was observed for NH₃ evolving from both fibers P1 and P2. The amount of the generated NH₃ gas from P2 fibers is much less than that of fibers P1. According to Hay et al. [21], ammonia is produced either in aromatization of the propagating cyclized unit or in the chance interaction of two propagating species. As a result, the accumulation of ammonia may reflect the occurring of cyclization termination of PAN. The fibers P2 produce less amount of NH₃ in the whole degradation process, suggesting that a more extensive intra-molecular cyclization structure (with a low termination probability) was formed in the sample. This is consistent with the results from thermal shrinkage analysis.

Evaluation on mechanical properties for oxidized fibers and carbon fibers

The mechanical properties of two kinds of PAN precursor fibers and the corresponding carbon fibers are tabulated in Table 3.

The oxidized fibers and carbon fibers have the identical labels with precursor fibers. For carbon fibers P1 and P2, the difference in mechanical properties is slight; however, the oxidized fibers have truly different properties. It can be seen that the mechanical properties (tensile strength, elastic modulus and strain to failure) of oxidized fiber P2 appeared to be about one-half of oxidized fiber P1. Obviously, the two precursors have distinct fiber structures after oxidative stabilization. As described before [22, 23], the tensile test of oxidized PAN fibers is an indication of the degree of cyclization. In other words, the decrease in tensile strength of oxidized fibers is due to the loss of inter-chain cohesive energy as result of intra-molecular cyclization reactions [24]. With this in mind, it should be indicated that the oxidized fibers P2 may have a greater degree of cyclization than oxidized fibers P1. The cyclization mechanism for PAN/AAM copolymer (shown in Fig. 10) proposed by Sivy et al. [17] indicate that except for the NH induced cyclization, the PAN/AAM samples can further propagate in another direction induced by the exocyclic hydroxyl group; instead, the reactions in P1 occurs in only one direction by NH initiation. Analogous to PAN/AAM copolymer, the P2 samples produce an average more extensive ring structure, as evidenced by results from tensile test, TG–MS and thermal shrinkage behavior analysis.

Table 3 The properties of oxidized and carbonized fibers

Specimens	Linear Density (g/m)	Volume Density (g/cm ³)	Tenacity (GPa)	Modulus (GPa)	Elongation at failure (%)
Oxidized fibers					
P1	0.3797	1.374	0.346	6.70	10.61
P2	0.3650	1.375	0.151	3.24	5.32
Carbon fibers					
P1	0.2029	1.775	3.94	211.2	1.99
P2	0.1981	1.784	3.92	218.0	1.97

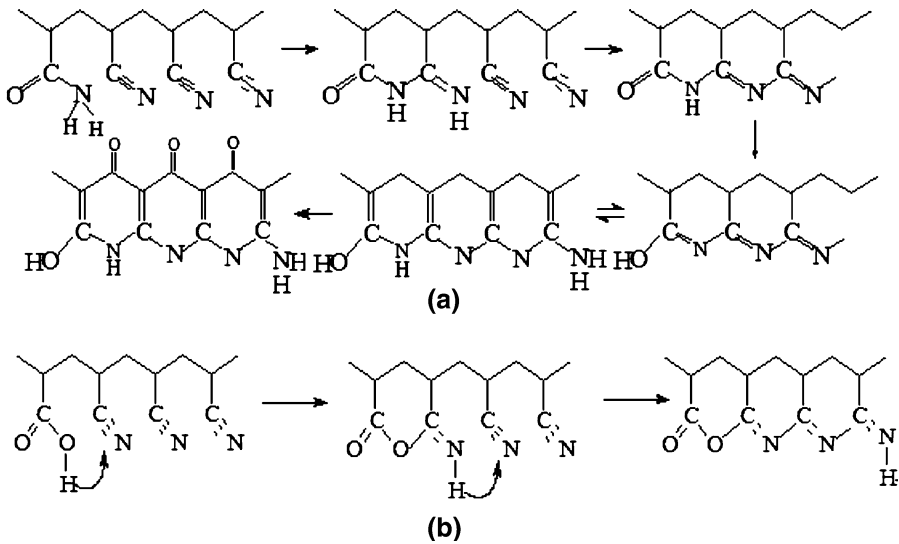


Fig. 10 Mechanism of cyclization initiation in air for (a) PAN/AAM copolymers and (b) PAN with carboxyl comonomers

Conclusion

1. Compared with PAN/ITA copolymer, PAN/AAM samples produce more extensive ring structure in the thermal stabilization or degradation process, as evidenced by results from tensile test, TG–MS and thermal shrinkage behavior analysis.
2. The precursor fibers containing AAM copolymers show a doublet appearance, broad exothermic peak, low threshold degradation temperature, and more amount of heat evolved in DSC thermogram. This is favorable to obtain uniform microstructures after oxidative stabilization.
3. In modulated DSC thermogram, the reversing contribution associated with molecular rearrangement or melting in crystalline structures is detected in a temperature in which nitrile cyclization is initiated simultaneously. The reversing contribution in amorphous and crystalline regions corresponds to molecular rearrangement and crystal melting, respectively.

Acknowledgments The authors wish to acknowledge financial support from Key Program of National Natural Science Foundation of China, grant number: 50333070.

References

1. Bashir Z (1999) A critical review of the stabilisation of polyacrylonitrile. *Carbon* 29:1081–1090
2. Yu MJ, Wang CG, Bai YJ et al (2008) Effect of oxygen uptake and aromatization on the skin-core morphology during the oxidative stabilization of polyacrylonitrile fibers. *J Appl Polym Sci* 107:1939–1945

3. Hou Y, Sun T, Wang H et al (2008) A new method for the kinetic study of cyclization reaction during stabilization of polyacrylonitrile fibers. *J Mater Sci* 43:4910–4914
4. Jing M, Wang CG, Bai YJ et al (2007) Effect of temperatures in the rearmost stabilization zone on structure and properties of PAN-based oxidized fibers. *Polym Bull* 58:541–551
5. Rahaman MSA, Ismail AF, Mustafa A (2007) A review of heat treatment on polyacrylonitrile fiber. *Polym Degrad Stab* 92:1421–1432
6. Wu G, Lu C, Ling L et al (2005) Influence of tension on the oxidative stabilization process of polyacrylonitrile fibers. *J Appl Polym Sci* 96:1029–1034
7. Warner SB, Peebles LH, Uhlmann DR (1979) Oxidative stabilization of acrylic fibres. Part 1 Oxygen uptake and general mode. *J Mater Sci* 14:556–564
8. Bahl OP, Manocha LM (1974) Characterization of oxidized PAN fibres. *Carbon* 12:417–423
9. Yu M, Wang C, Bai Y et al (2006) Influence of precursor properties on the thermal stabilization of polyacrylonitrile fibers. *Polym Bull* 57:757–763
10. Bahl OP, Shen Z, Lavin JG et al (1998) Manufacture of carbon fibers. In: Donnet JB, Wang TK, Peng JM et al (eds) *Carbon fibers*, 3rd edn. Marcel Dekker, New York, pp 1–83
11. Zhang W, Liu J, Wu G (2003) Evolution of structure and properties of PAN precursors during their conversion to carbon fibers. *Carbon* 41:2805–2812
12. Mauerer A, Lee G (2006) Changes in the amide I FT-IR bands of poly-L-lysine on spray drying from the alpha-helix, beta-sheet or random coil conformations. *Eur J Pharm Biopharm* 62:131–142
13. Tsai JS (1993) Modes of stress-strain curve distribution for modacrylic fibres. *J Mater Sci* 28:4841–4845
14. Mittal J, Mathur RB, Bahl OP et al (1998) Post spinning treatment of PAN fibers using succinic acid to produce high performance carbon fibers. *Carbon* 36:893–897
15. Simitzis J, Soulis S (2008) Correlation of chemical shrinkage of polyacrylonitrile fibres with kinetics of cyclization. *Polym Inter* 57:99–105
16. Surianarayanan M, Vijayaraghavan R, Raghavan KV et al (1998) Spectroscopic investigations of polyacrylonitrile thermal degradation. *J Polym Sci A* 36:2503–2512
17. Sivy GT, Coleman MM (1981) Fourier transform IR studies of the degradation of polyacrylonitrile copolymers-IV acrylonitrile/acrylamide copolymers. *Carbon* 19:137–139
18. Raskovic V, Marinkovic S (1975) Temperature dependence of processes during oxidation of PAN fibres. *Carbon* 13:535–538
19. Gupta A, Harrison IR (1996) New aspects in the oxidative stabilization of PAN-based carbon fibers. *Carbon* 34:1427–1445
20. Ko TH, Lin CH, Ting HY (1989) Structural changes and molecular motion of polyacrylonitrile fibers during pyrolysis. *J Appl Polym Sci* 37:553–556
21. Hay JN (1968) Thermal reactions of polyacrylonitrile. *J Polym Sci A* 6:2127–2135
22. Wu G, Lu C, Zhang R et al (2004) Effect of moisture on stabilization of polyacrylonitrile fibers. *J Mater Sci* 39:2959–2960
23. Mathur RB, Mittal J, Bahl OP (1993) Biomodification of polyacrylonitrile (PAN) fibers. *J Appl Polym Sci* 49:469–476
24. Gupta A, Harrison IR (1997) New aspects in the oxidative stabilization of PAN-based carbon fibers: II. *Carbon* 35:809–818